MATHEMATICAL MODELING AND COMPUTING, Vol. 10, No. 4, pp. 1037–1050 (2023)

Viral infection model with cell-to-cell transmission and therapy in the presence of humoral immunity: Global analysis

El Akraa N.[1], Lahby M.[1], Danane J.[2]

[1] *Laboratory of Mathematics and Applications, University Hassan II, Higher Normal School of Casablanca, Casablanca, Morocco*
[2] *Laboratory of Systems, Modelization and Analysis for Decision Support, National School of Applied Sciences, Hassan First University, Berrechid, Morocco*

(Received 12 February 2023; Revised 24 September 2023; Accepted 19 November 2023)

This paper aims to prezent mathematical model for Viral infection which incorporates both the cell-free and cell-to-cell transmission. The model includes four compartments, namely, the susceptible, the infected ones, the viral load and the humoral immune response, which is activated in the host to attack the virus. Firstly, we establish the well-posedness of our mathematical model in terms of proving the existence, positivity and boundedness of solutions. Moreover, we determine the different equilibrium of the problem. Also, we will study the global stability of each equilibrium. Finally, we give some numerical simulation in order to validate our theoretical findings, and to study the effect of different types of treatments proposed by the model.

Keywords: *global stability; cell-to-cell; humoral immune response; therapy; basic reproduction number; numerical simulation.*

2010 MSC: 34A12, 34D20, 37M05, 92-08, 92-10 **DOI:** 10.23939/mmc2023.04.1037

1. Introduction

Nowadays infectious diseases threaten the life of millions of people on earth. Amongst the well known viruses, one can cite the human papillomavirus (HPV) that infects the basal cells of the cervix [1, 2], the human immunodeficiency virus (HIV) that attacks the healthy CD4+ immune system [3, 4], the hepatitis B virus (HBV) and the hepatitis C virus (HCV) that attacks the uninfected liver cells [5–8] and more recently the Coronavirus Disease 2019 (COVID-19) [9–11]. Therefore, mathematical modeling has become very important to study how diseases spread, and also to predict the future trajectory of an outbreak, which can help the public health authorities to take the necessary measures [12, 13]. In 1998 Neumann et al. proposed a model that describes the dynamics of transmission of HCV by reference to a simple interaction between the susceptible cells, infected cells and virions [14]. Neumann et al.'s model postulates that virus-to-cell transfer is responsible for the infection; in other words, the infection occurs due to the contact between susceptible cells and free virions with a bilinear incidence rate. Since disease can spread through the body through virus-to-cell infection or by direct virus transfer from cell to cell [15], many research provided mathematical models by integrating two modes of infection transmission [16–18]. To have a relevant mathematical modeling it is necessary to take into consideration the effect of the humoral immunity of the human body indeed, immediately after infection, the immune system of the host body acts against the virus by activating adaptive immunity, which is called destroy pathogens. This system recognizes the different types of pathogens and calls for the most effective form of adaptive immune response to destroy them [19, 20]. Also, the treatment can play an important role against the spread of different viral infections [21, 22].

This paper includes three treatments to decrease the production of virions from infected cells, and to reduce the infection caused by virus-to-cell and cell-to-cell transmission, so the dynamics of virus transmission can be described using the following model:

$$\begin{cases} \dfrac{dT}{dt} = \lambda - (1-u_1)\beta_1 TV - (1-u_2)\beta_2 TI - d_1 T, \\ \dfrac{dI}{dt} = (1-u_1)\beta_1 TV + (1-u_2)\beta_2 TI - d_2 I, \\ \dfrac{dV}{dt} = (1-u_3)kI - d_3 V - pVZ, \\ \dfrac{dZ}{dt} = cVZ - d_4 Z, \end{cases} \tag{1}$$

where the initial data are $(T(0), I(0), V(0), Z(0)) = (T_0, I_0, V_0, Z_0)$, with $T(t)$, $I(t)$, $V(t)$, $Z(t)$ populations of uninfected cells, infected cells, virus-free particles, and humoral immune response respectively, sensitive cells are assumed to reproduce with a constant rate λ, the average lifespan of sensitive cells, infected, free virus and immune cells are $1/d_1$, $1/d_2$, $1/d_3$, and $1/d_4$ respectively, cell-to-virus and cell-to-cell infection occur with β_1 and β_2 rate respectively, free virions are produced at a rate of k per infected cell, the coefficients u_3, u_1, and u_2 represent three treatments to decrease the production of virions from infected cells, and to reduce the infection caused by virus-to-cell and cell-to-cell transmission, after entry of virions, the humoral immune response is activated at a rate c per virion, and virions are neutralized at a rate p per virion.

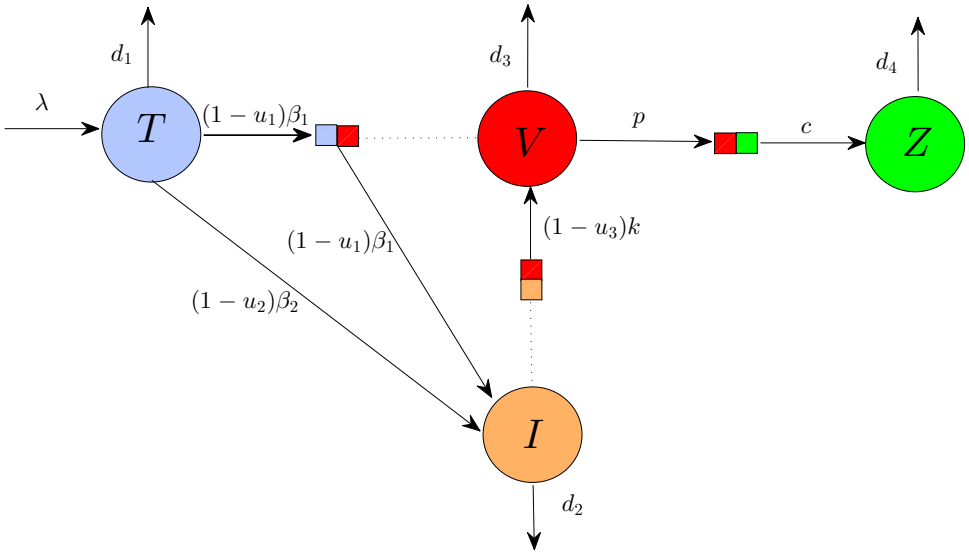

Fig. 1. Diagram describing the model.

The present work is organized as follows, the next section is dedicated to prove the non-negativity and boundedness of solutions. Section 3 gives the mathematical results about existence and stability of equilibria and finally in section 4 we represent numerical tests. The last section concludes the work.

2. Non-negativity and boundedness of solutions

Theorem 1. *The system solutions* (1) *with the initial state in* $\mathbb{R}_4^+$ *are positive and bounded. In addition, there is a* $\varepsilon > 0$ *such as* $\liminf_{t\to+\infty} T(t) \geqslant \varepsilon$.

Proof. According to the system (1) we have

$$\left.\frac{dT}{dt}\right|_{T=0} = \lambda + \alpha I, \quad \left.\frac{dI}{dt}\right|_{I=0} = (1-u_1)\beta_1 TV, \quad \left.\frac{dV}{dt}\right|_{V=0} = (1-u_3)kI.$$

Suppose there is $t > 0$ such as $\left.\frac{dV(t)}{dt}\right|_{V(t)=0} < 0$, we note

$$t_v = \inf\left\{ t > 0 / V(t) = 0 \text{ and } \left.\frac{dV(t)}{dt}\right|_{V(t)=0} < 0 \right\}.$$

Therefore $\frac{dV(t_v)}{dt}\Big|_{V(t_v)=0} = (1-u_3)kI(t_v) < 0$ now let define

$$t_I = \inf\left\{t > 0/I(t) = 0 \text{ and } \frac{dI(t)}{dt}\Big|_{I(t)=0} < 0\right\}.$$

We deduce that $t_I < t_v$, therefore $\frac{dI(t_I)}{dt}\Big|_{I(t_I)=0} = (1-u_1)\beta_1 T(t_I)V(t_I) < 0$ which implies that $T(t_I) < 0$ since $V(t_I) > 0$. Let us define

$$t_T = \inf\left\{t > 0/T(t) = 0 \text{ and } \frac{dT(t)}{dt}\Big|_{T(t)=0} < 0\right\}.$$

We have $t_T < t_I < t_V$ and $\frac{dT(t_T)}{dt}\Big|_{T(t_T)=0} = \lambda + \alpha I(t_T) > 0$ since $I(t_T) > 0$ which contradicts the definition of t_T.

Therefore $\frac{dV}{dt}\big|_{V=0} \geqslant 0$ thus $V(t) \geqslant 0$, $\forall t > 0$ consequently $I(t) \geqslant 0$, $T(t) \geqslant 0$, $\forall t > 0$.

Finally according to the last equation of the system (1) we find

$$Z(t) = Z(0)\exp\left\{\int_0^t \big[cV(s) - d_4\big]ds\right\} \geqslant 0 \quad \forall t \geqslant 0.$$

Therefore, the non-negativity of the solutions with the initial condition in $\mathbb{R}_4^+$ is guaranteed.

To prove the boundfulness of the system solutions (1), we define two new variables $X(t) = T(t)+I(t)$ and $Y(t) = V(t)+pcZ(t)$. From the first two equations of (1), we obtain $\frac{dX(t)}{dt} = \lambda - d_1T(t) - d_2I(t) \leqslant \lambda - d_xX(t)$ such as $d_x = \min\{d_1, d_2\}$. Therefore $\limsup_{t\to+\infty} X(t) \leqslant \frac{\lambda}{d_x}$.

Moreover according to the last equations of the system (1) (1) $\frac{dY(t)}{dt} = (1-u_3)kI(t) - d_3V(t) - \frac{d_4P}{c}Z(t) \leqslant (1-u_3)kI(t) - d_YY(t)$ such as, $d_Y = \min\{d_3, d_4\}$ therefore, $\limsup_{t\to+\infty} Y(t) \leqslant \frac{\lambda(1-u_3)k}{d_xd_Y}$. Thus, the solutions of system (1) with non-negative initial conditions are bounded by the set

$$D = \left\{(T(t), I(t), V(t), Z(t)) \in \mathbb{R}_+^4 : 0 \leqslant T(t), I(t) \leqslant \frac{\lambda}{d_x}; \right.$$
$$\left. 0 \leqslant V(t) \leqslant \frac{\lambda(1-u_3)k}{d_xd_y}; 0 \leqslant Z(t) \leqslant \frac{c\lambda(1-u_3)k}{pd_xd_y}\right\}.$$

Moreover, from the first equation of the system (1), we obtain

$$\begin{aligned}\frac{dT(t)}{dt} &\geqslant \lambda - (1-u_1)\beta_1T(t)V(t) - (1-u_2)\beta_2T(t)I(t) - d_1T(t)\\ &\geqslant \lambda - (d_1 + (1-u_1)\beta_1V_u + (1-u_2)\beta_2I_u)T(t) \quad \text{for} \quad t \quad \text{big enough}\end{aligned}$$

where $I_u = \frac{\lambda}{d_x}$ and $V_u = \frac{\lambda(1-u_3)k}{d_xd_y}$ are two upper limits of $I(t)$ and $V(t)$, respectively . Therefore $\liminf_{t\to+\infty} T(t) \geqslant \frac{\lambda}{d_1+(1-u_1)\beta_1V_u+(1-u_2)\beta_2I_u}$. It follows that there is a $\varepsilon > 0$ such as $\liminf_{t\to+\infty} T(t) \geqslant \varepsilon$. ∎

3. Existence and stability of equilibria

3.1. Existence of equilibria

The system (1) accepts three points of equilibrium:

— The point of equilibrium with no disease $E_0 = (T_0, I_0, V_0, Z_0)$ where: $T_0 = \frac{\lambda}{d_1}$ and $I_0 = V_0 = Z_0 = 0$.

— Free immune equilibrium $E_1 = (T_1, I_1, V_1, Z_1)$ where: $T_1 = \frac{d_3d_2}{(1-u_1)\beta_1(1-u_3)k+(1-u_2)\beta_2d_3}$ and $I_1 = \frac{d_1T_1}{d_2}\left[\frac{\lambda((1-u_1)\beta_1(1-u_3)k+(1-u_2)\beta_2d_3)}{d_1d_3d_2} - 1\right]$ and $V_1 = \frac{(1-u_3)k}{d_3}I_1$, $Z_1 = 0$.

— Infected equilibrium with immune response $E_2 = (T^*, I^*, V^*, Z^*)$,

$$T^* = \frac{d_2I^*}{(1-u_2)\beta_2V^* + (1-u_2)\beta_2I^*}, \quad I^* = \frac{-m_2 + \sqrt{m_2^2 + 4m_1m_3}}{2m_1},$$

$$V^* = \frac{d_4}{c}, \quad Z^* = \frac{d_3}{p}\left(\frac{c(1-u_3)k}{d_3 d_4} I^* - 1\right)$$

where: $m_1 = (1-u_2)\beta_2 c d_2$, $m_2 = (1-u_1)\beta_1 d_2 d_4 + c d_1 d_2 - \lambda(1-u_2)\beta_2 c$, $m_3 = \lambda(1-u_1)\beta_1 d_4$.

In order to determine the expression of the basic reproduction number, we apply the next generation matrix approach [23]. Accordingly, the equations associated with infection are:

$$\begin{cases} \dfrac{dI}{dt} = (1-u_1)\beta_1 TV + (1-u_2)\beta_2 TI - d_2 I, \\ \dfrac{dV}{dt} = (1-u_3)kI - d_3 V - pVZ. \end{cases} \tag{2}$$

So, the matrices describing the speed of infection in the compartments, and the speed of virus transfer out of compartments are

$$\mathcal{F} = \begin{pmatrix} (1-u_1)\beta_1 TV + (1-u_2)\beta_2 TI \\ 0 \end{pmatrix}, \quad \mathcal{V} = \begin{pmatrix} d_2 I \\ -(1-u_3)kI + d_3 V + pVZ \end{pmatrix}.$$

Therefore

$$F = J_{\mathcal{F}}(Q_0) = \begin{pmatrix} \frac{\lambda(1-u_2)\beta_2}{d_1} & \frac{\lambda(1-u_1)\beta_1}{d_1} \\ 0 & 0 \end{pmatrix}$$

and

$$V = J_{\mathcal{V}}(Q_0) = \begin{pmatrix} d_2 & 0 \\ -(1-u_3)k & d_3 \end{pmatrix}.$$

We have

$$V^{-1} = \frac{1}{d_2 d_3}\begin{pmatrix} d_3 & 0 \\ (1-u_3)k & d_2 \end{pmatrix}.$$

Finally

$$\begin{aligned} R_0 = \rho(FV^{-1}) &= \frac{\lambda((1-u_1)\beta_1(1-u_3)k + (1-u_2)\beta_2 d_3)}{d_1 d_3 d_2} \\ &= \frac{(1-u_3)k(1-u_1)\beta_1 T_0}{d_3 d_2} + \frac{(1-u_2)\beta_2 T_0}{d_2} \\ &= R_{01} + R_{02}, \end{aligned}$$

where $R_{01} = \frac{(1-u_3)k(1-u_1)\beta_1 T_0}{d_3 d_2}$ and $R_{02} = \frac{(1-u_2)\beta_2 T_0}{d_2}$ are the basic reproductive numbers for virus-to-cell and cell-to-cell infections (resp), [24].

We define a new threshold parameter $R_1 = \frac{c(1-u_3)k}{d_3 d_4} I^*$, representing the number of viral reproduction in the chronic stage of infection without the effect of the humoral immune response to virions.

We also define the humoral immune reproduction number as follows:

$$R_H = \frac{c(1-u_3)k\lambda((1-u_1)\beta_1(1-u_3)k + (1-u_2)\beta_2 d_3)}{c(1-u_3)k d_1 d_3 d_2 + d_2 d_3 d_4((1-u_1)\beta_1(1-u_3)k + (1-u_2)\beta_2 d_3)}.$$

Which represents the average number of infected secondary cells produced in the presence of a humoral immune response.

Lemma 1. *(i) $R_1 > 1 \Longleftrightarrow R_H > 1$; (ii) $R_1 = 1 \Longleftrightarrow R_H = 1$; (iii) $R_1 < 1 \Longleftrightarrow R_H < 1$.*

Proof. For (i) we have

$$\begin{aligned} R_1 > 1 &\Longleftrightarrow I^* > \frac{d_3 d_4}{c(1-u_3)k}, \\ &\Longleftrightarrow \frac{-m_2 + \sqrt{m_2^2 + 4m_1 m_3}}{2m_1} > \frac{d_3 d_4}{c(1-u_3)k}, \\ &\Longleftrightarrow (m_2^2 + 4m_1 m_3) - \left(\frac{2m_1 d_3 d_4}{c(1-u_3)k} + m_2\right)^2 > 0. \end{aligned}$$

By simplifying we find that

$R_1 > 1 \iff$

$$\frac{4(1-u_1)\beta_1 d_2 d_4}{(1-u_3)k^2}[c(1-u_3)kd_1d_3d_2 + d_2d_3d_4((1-u_1)\beta_1(1-u_3)k + (1-u_2)\beta_2 d_3)](R_H - 1) > 0,$$

therefore $R_1 > 1 \iff R_H > 1$, similarly we show (ii) and (iii).

And since $R_H < R_0$ we have $R_0 < 1 \implies R_1 < 1$ and, $R_1 > 1 \implies R_0 > 1$. ∎

4. Stability of equilibria

To discuss the global behavior of the system (1), we adopt the method of Lyapunov functionals and use the Lyapunov–LaSalle invariance principle [25].

Theorem 2. *The disease-free equilibrium E_0 is globally asymptotically stable when $R_0 \leqslant 1$.*

Proof. Considering the following Lyapunov function

$$L_1(T, I, V, Z) = T_0\left(\frac{T}{T_0} - 1 - \ln\frac{T}{T_0}\right) + I + \frac{(1-u_1)\beta_1 T_0}{d_3}V + \frac{(1-u_1)\beta_1 p T_0}{cd_3}Z.$$

Its derivative is

$$\begin{aligned}\frac{dL_1}{dt} &= T_0 d_1\left(2 - \frac{T}{T_0} - \frac{T_0}{T}\right) + (1-u_2)\beta_2 T_0 I - d_2 I + \frac{(1-u_1)\beta_1 T_0(1-u_3)kI}{d_3} - \frac{(1-u_1)\beta_1 p T_0 d_4 Z}{cd_3}\\ &= T_0 d_1\left(2 - \frac{T}{T_0} - \frac{T_0}{T}\right) + d_2 I(R_0 - 1) - \frac{(1-u_1)\beta_1 p T_0 d_4 Z}{cd_3}.\end{aligned}$$

Note M_a and M_g the arithmetic and geometric means (resp) of two numbers $\frac{T}{T_0}$ and $\frac{T_0}{T}$, we have $M_g < M_a$ thus $(2 - (T/T_0 + T_0/T)) \leqslant 0$.

Therefore $\frac{dL_1}{dt} \leqslant 0$ when $R_0 \leqslant 1$. Let M_0 be the largest invariant set $M_0 = \left\{(T, I, V, Z)/\frac{dL_1}{dt} = 0\right\}$ we note that $\frac{dL_1}{dt} = 0$ if and only if $T = T_0$ and $I = 0$ and $Z = 0$ and $V = 0$, thus $M_0 = E_0$, based on LaSalle's invariance principle, E_0 is globally asymptotically stable if $R_0 \leqslant 1$. ∎

Theorem 3. *The immune free equilibrium E_1 is globally asymptotically stable when $R_1 \leqslant 1 < R_0$.*

Proof. Considering the following Lyapunov function

$$\begin{aligned}L_2(T, I, V, Z) = T_1\left(\frac{T}{T_1} - 1 - \ln\frac{T}{T_1}\right) + I_1\left(\frac{I}{I_1} - 1 - \ln\frac{I}{I_1}\right)\\ + \frac{(1-u_1)\beta_1 T_1 V_1^2}{(1-u_3)kI_1}\left(\frac{V}{V_1} - 1 - \ln\frac{V}{V_1}\right) + \frac{(1-u_1)\beta_1 p T_1 V_1}{c(1-u_3)kI_1}Z.\end{aligned}$$

Its time derivative is

$$\begin{aligned}\frac{dL_2}{dt} &= -d_1 T_1\frac{(T-T_1)^2}{TT_1} - (1-u_1)\beta_1 T_1 V_1\left(\frac{T_1}{T} + \frac{IV_1}{I_1 V} + \frac{TI_1 V}{T_1 IV_1} - 3\right)\\ &= -(1-u_2)\beta_2 T_1 I_1\left(\frac{T}{T_1} + \frac{T_1}{T} - 2\right) + \frac{\lambda(1-u_1)\beta_1(1-u_3)kpT_1 Z}{d_2 d_3^2 R_H}(R_H - 1).\end{aligned}$$

Since arithmetic mean is greater than geometric mean we have, $\frac{dL_2}{dt} \leqslant 0$ when $R_H \leqslant 1$ thus $R_1 \leqslant 1$ according to the lemma. Let be M_1 the largest invariant set such as

$$M_1 = \left\{(T, I, V, Z)/\frac{dL_2}{dt} = 0\right\}.$$

We have $\frac{dL_2}{dt} = 0$ if and only if $T = T_1$, $I = I_1$, $Z = Z_1$ and $V = V_1$, thus $M_1 = \{E_1\}$, so based on LaSalle's invariance principle, E_1 is globally asymptotically stable if $R_1 \leqslant 1$. And as E_1 exists whenever $R_0 > 1$, we find the result of the theorem. ∎

Theorem 4. *The infected equilibrium with humoral immune response E_2 is locally asymptotically stable when $R_1 > 1$.*

Proof. Considering the following Lyapunov function

$$L_3(T,I,V,Z) = T^*\left(\frac{T}{T^*} - 1 - \ln\frac{T}{T^*}\right) + I^*\left(\frac{I}{I^*} - 1 - \ln\frac{I}{I^*}\right) + \frac{(1-u_1)\beta_1 T^* V^{*2}}{(1-u_3)kI^*}\left(\frac{V}{V^*} - 1 - \ln\frac{V}{V^*}\right) + \frac{(1-u_1)\beta_1 pT^*V^*Z^*}{c(1-u_3)kI^*}\left(\frac{Z}{Z^*} - 1 - \ln\frac{Z}{Z^*}\right).$$

Its time derivative is

$$\frac{dL_3}{dt} = -d_1T^*\frac{(T-T^*)^2}{TT^*} - (1-u_1)\beta_1 T^*V^*\left[\frac{T^*}{T} + \frac{IV^*}{I^*V} + \frac{TI^*V}{T^*IV^*} - 3\right] - (1-u_2)\beta_2 T^*I^*\left[\frac{T}{T^*} + \frac{T^*}{T} - 2\right].$$

Let be M^* the largest invariant set such as

$$M^* = \left\{(T,I,V,Z)/\frac{dL_3}{dt} = 0\right\}.$$

We have $\frac{dL_3}{dt} = 0$ if and only if $T = T^*$, $I = I^*$, $Z = Z^*$ and $V = V^*$, thus $M^* = E_2$, and since E_2 exists whenever $R_1 > 1$, so based on the invariance principle of LaSalle E_2 is globally asymptotically stable if $R_1 > 1$. ■

5. Numerical simulations

In this section, we present several numerical illustrations for the model (1) in order to validate our theoretical findings, and also to study the effectiveness of different therapys offered by the model.

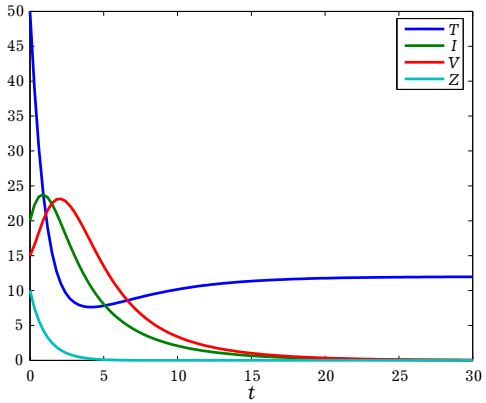

Fig. 2. The dynamics of the infection when $\lambda = 6$, $\beta_1 = 0.01$, $\beta_2 = 0.01$, $d_1 = 0.5$, $d_2 = 0.5$, $d_3 = 0.8$, $d_4 = 0.9$, $k = 0.9$, $p = 0.006$, and $c = 0.005$.

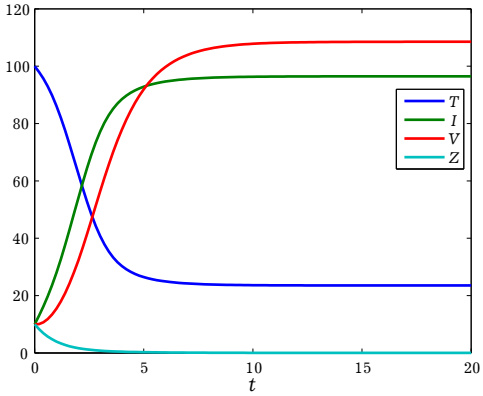

Fig. 3. The behavior of the infection when $\lambda = 60$, $\beta_1 = 0.01$, $\beta_2 = 0.01$, $d_1 = 0.5$, $d_2 = 0.5$, $d_3 = 0.8$, $d_4 = 0.9$, $k = 0.9$, $p = 0.006$, and $c = 0.005$.

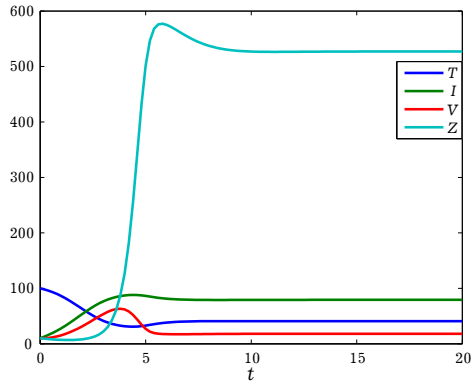

Fig. 4. The dynamics of the infection when $\lambda = 60$, $\beta_1 = 0.01$, $\beta_2 = 0.01$, $d_1 = 0.5$, $d_2 = 0.5$, $d_3 = 0.8$, $d_4 = 0.9$, $k = 0.9$, $p = 0.006$, and $c = 0.05$.

Figure 2 represents the behavior of the infection when $\lambda = 6$, $\beta_1 = 0.01$, $\beta_2 = 0.01$, $d_1 = 0.5$, $d_2 = 0.5$, $d_3 = 0.8$, $d_4 = 0.9$, $k = 0.9$, $p = 0.006$, and $c = 0.005$, that is implies that $R_0 = 0.51 < 1$ and $R_1 = 0.05 < 1$. We observe that the studied population converges to the free equilibrium $E_0 = (12, 0, 0, 0)$, then these results validate our theoretical finding.

Figure 3 represents the dynamics of the infection when $\lambda = 60$, $\beta_1 = 0.01$, $\beta_2 = 0.01$, $d_1 = 0.5$, $d_2 = 0.5$, $d_3 = 0.8$, $d_4 = 0.9$, $k = 0.9$, $p = 0.006$, and $c = 0.005$, that is implies that $R_0 = 05.1 > 1$ and $R_1 = 0.49 < 1$. We observe that the studied population converges to the free equilibrium $E_1 = (23.5, 96.47, 108.52, 0)$, then these results validate our theoretical finding.

In Figure 4, we show the interaction between the studied population when $\lambda = 60$, $\beta_1 = 0.01$, $\beta_2 = 0.01$, $d_1 = 0.5$, $d_2 = 0.5$, $d_3 = 0.8$, $d_4 = 0.9$, $k = 0.9$, $p = 0.006$, and $c = 0.05$, that is implies that $R_0 = 06.3 > 1$ and $R_1 = 5.1 > 1$. We observe that the studied population converges to the free equilibrium $E_2 = (40.74, 79.85, 18, 527.11)$, then these results validate our theoretical finding.

5.1. Effect of therapy u_1

This subsection will study the effect of therapy parameters u_1 on the dynamics of the model system for each equilibrium.

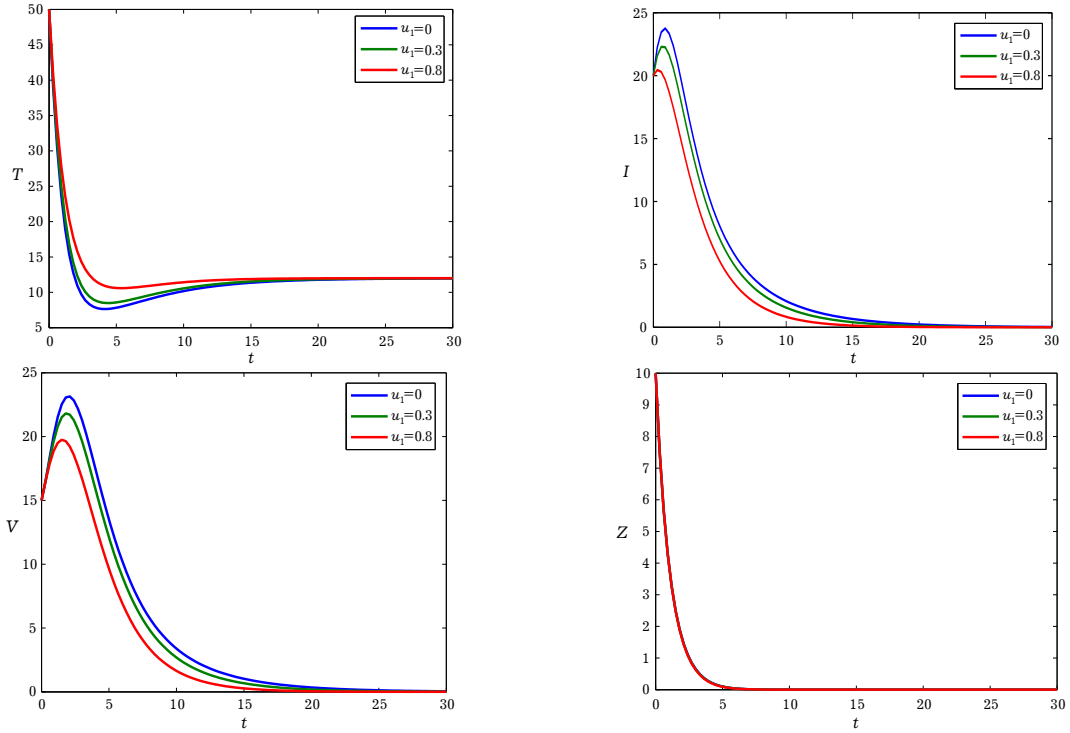

Fig. 5. Infection dynamics showing around the free equilibrium E_0 for different values of u_1.

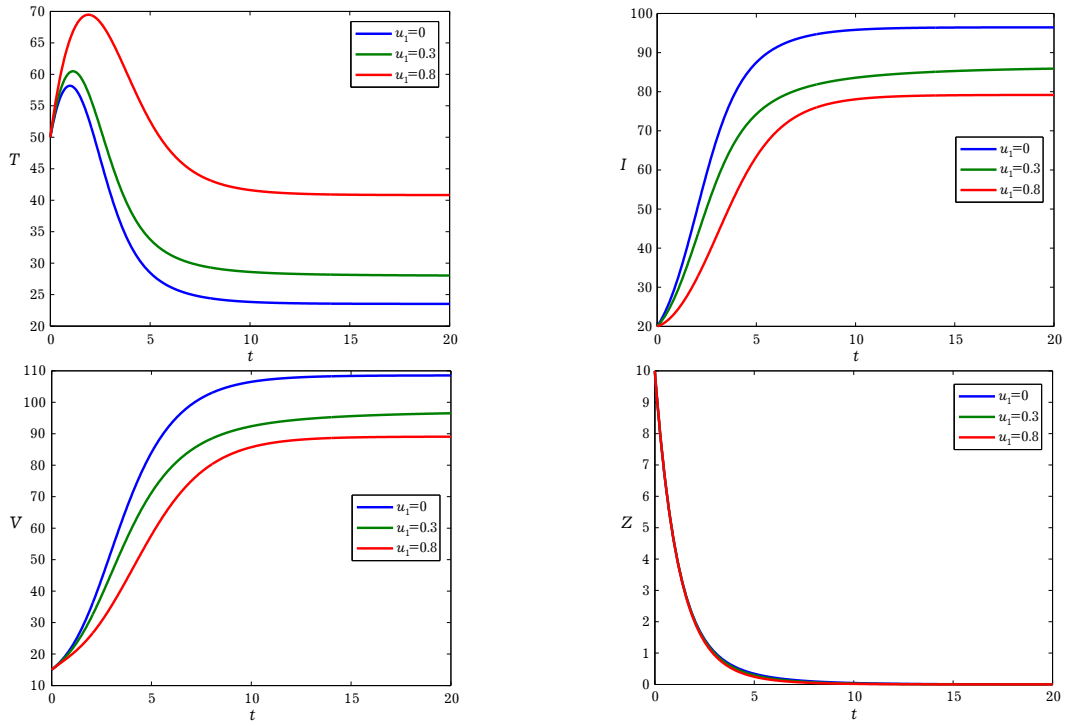

Fig. 6. Infection dynamics showing the stability of the E_1 for different values of u_1.

Figures 5 represent the effect of the therapy u_1 around the free equilibrium, we remark that when 30% and 80% on the first 5 days of treatment the uninfected cells decrease, after this period the uninfected cells increase to reach their equilibrium.

Figures 6 represent the effect of the therapy u_1 around the free immune endemic equilibrium E_1, we remark that when 30% and 80% the number of the uninfected cells increase on the contrary the number of the infected cells and the free virus decreases, that proves the efficiency of the therapy u_1.

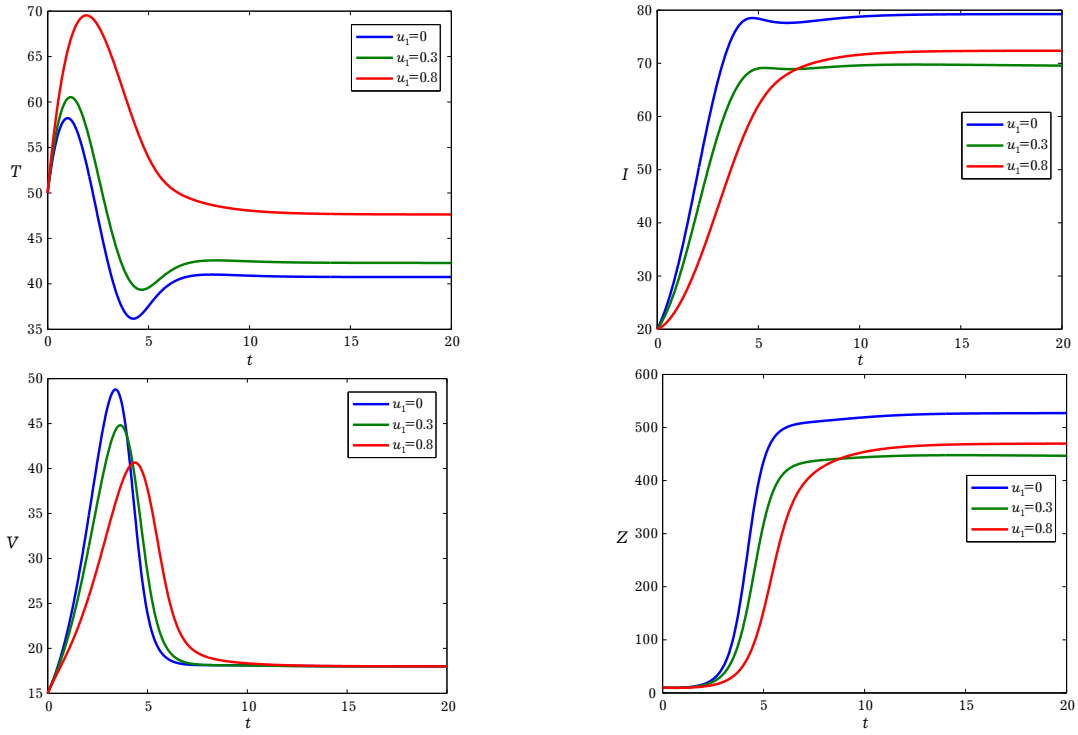

Fig. 7. Infection dynamics showing the stability of the E_2 for different values of u_1.

Figures 7 represent the effect of the therapy u_1 around the immune endemic equilibrium E_2, we remark that when 30% and 80% the number of the infected cells and the free virus decreases on the other hand we observe that the number of the uninfected cells increase, that proves the efficiency of the therapy u_1.

5.2. Effect of therapy u_2

In this subsection, we will study the effect of therapy parameters u_2 on the dynamics of the model system for each equilibrium.

Figures 8 represent the effect of the therapy u_2 around the free equilibrium, we remark that when 30% and 80% on the first days of treatment the uninfected cells decrease, after this period the uninfected cells increase to reach their equilibrium.

Figures 9 represent the effect of the therapy u_2 around the free immune endemic equilibrium E_1, we remark that when 30% and 80% the number of the uninfected cells increase on the contrary the number of the infected cells and the free virus decreases, that proves the efficiency of the therapy u_2.

Figures 10 represent the effect of the therapy u_2 around the immune endemic equilibrium E_2, we remark that when 30% and 80% the number of the infected cells and the free virus decreases on the other hand we observe that the number of the uninfected cells increase, that proves the efficiency of the therapy u_2.

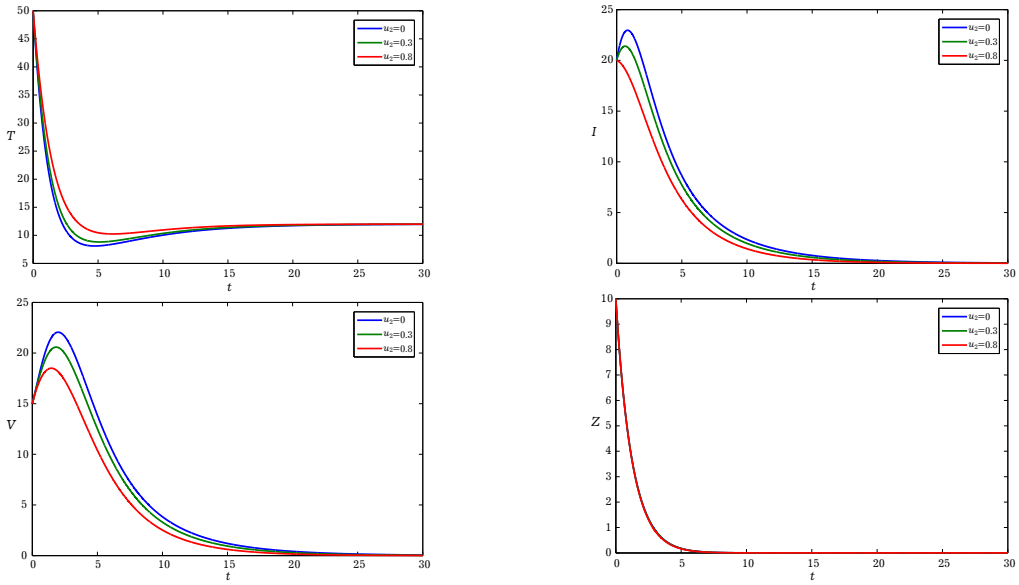

Fig. 8. Infection dynamics showing the stability of the E_0 for different values of u_2.

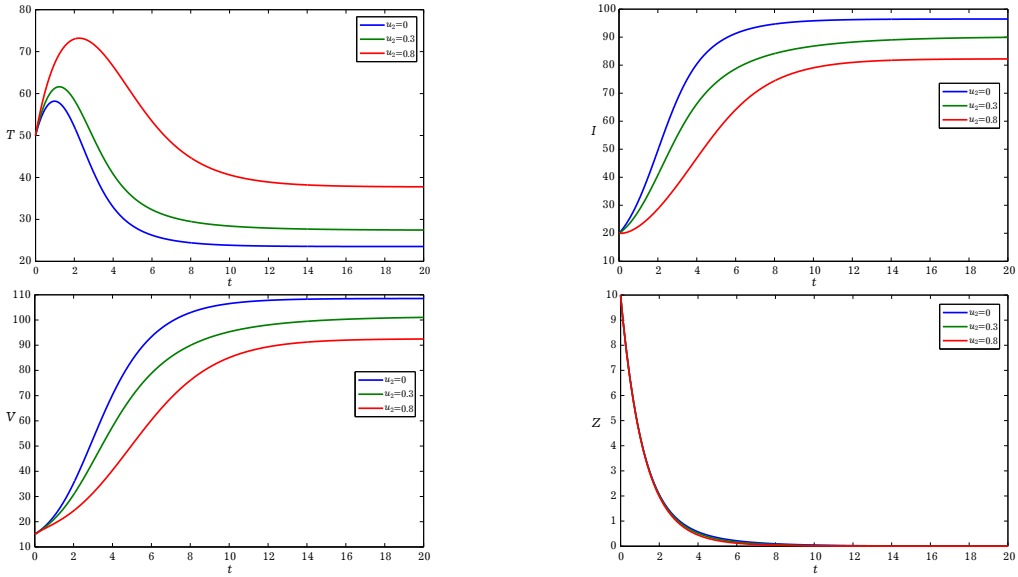

Fig. 9. Infection dynamics showing the stability of the E_1 for different values of u_2.

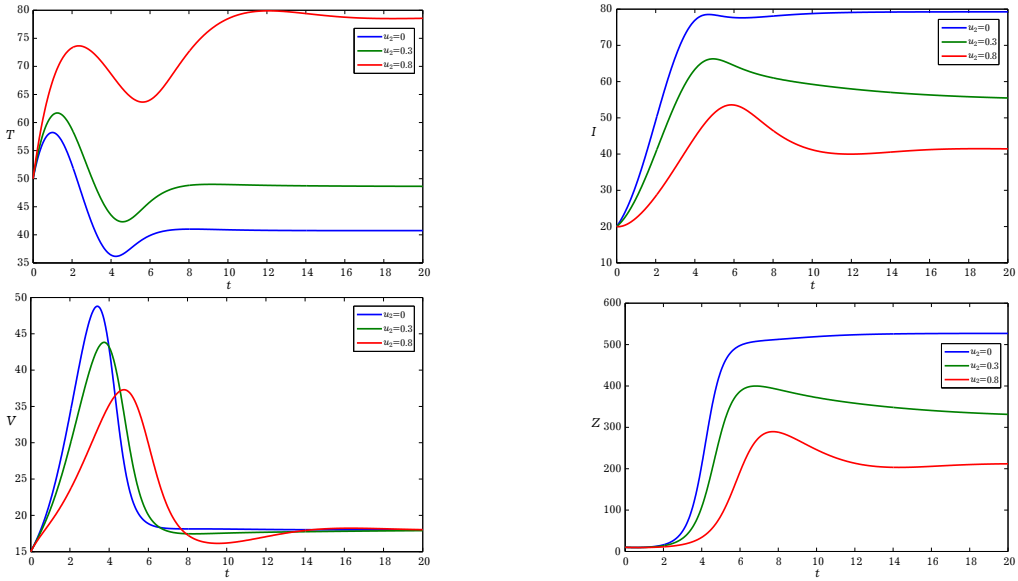

Fig. 10. Infection dynamics showing the stability of the E_2 for different values of u_2.

5.3. Effect of therapy u_3

In this subsection, we will study the effect of therapy parameters u_3 on the dynamics of the model system for each equilibrium.

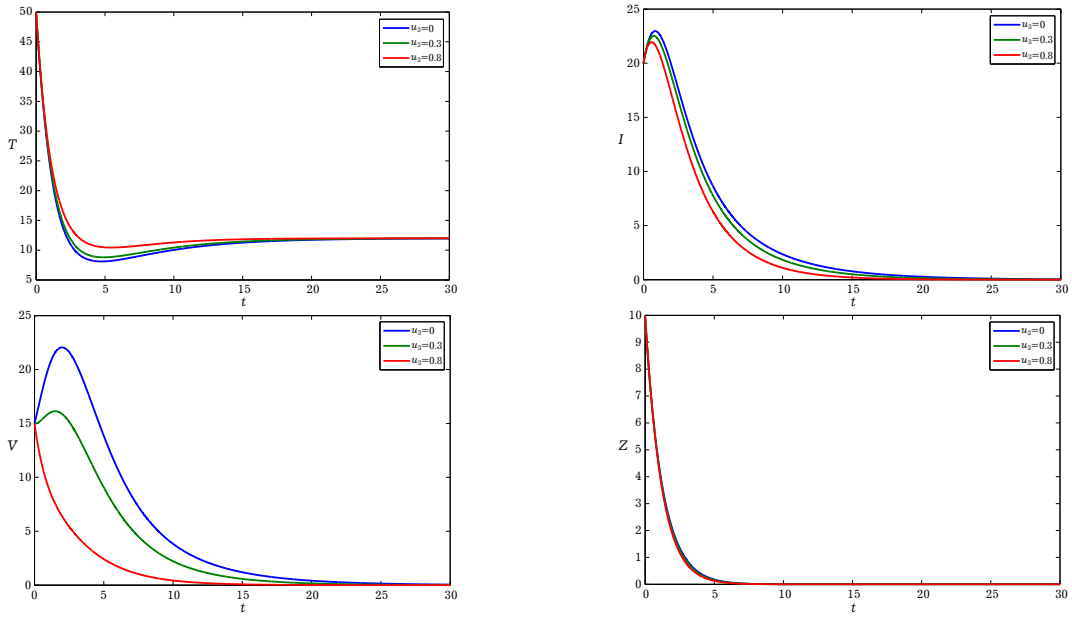

Fig. 11. Infection dynamics showing the stability of the E_0 for different values of u_3.

Figures 11 represent the effect of the therapy u_3 around the free equilibrium, we remark that when 30% and 80% on the first days of treatment the uninfected cells decrease, after this period the uninfected cells increase to reach their equilibrium.

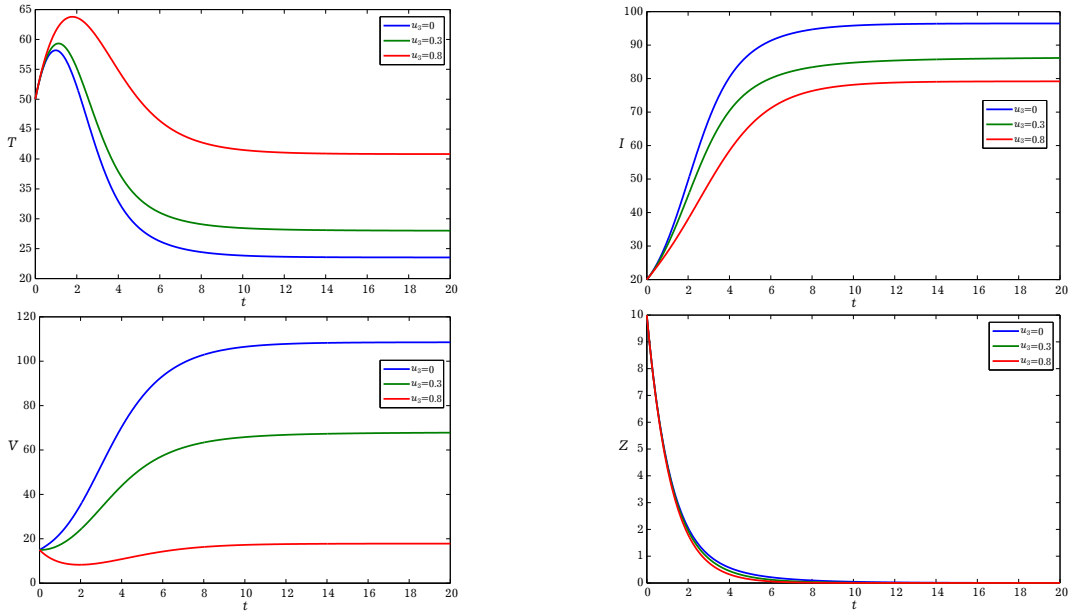

Fig. 12. Infection dynamics showing the stability of the E_1 for different values of u_3.

Figures 12 represent the effect of the therapy u_3 around the free immune endemic equilibrium E_1, we remark that when 30% and 80% the number of the uninfected cells increase on the contrary the number of the infected cells and the free virus decreases, that proves the efficiency of the therapy u_3.

Figures 13 represent the effect of the therapy u_3 around the immune endemic equilibrium E_2, we remark that when 30% and 80% the number of the infected cells and the free virus decreases on the other hand we observe that the number of the uninfected cells increase, that proves the efficiency of the therapy u_3.

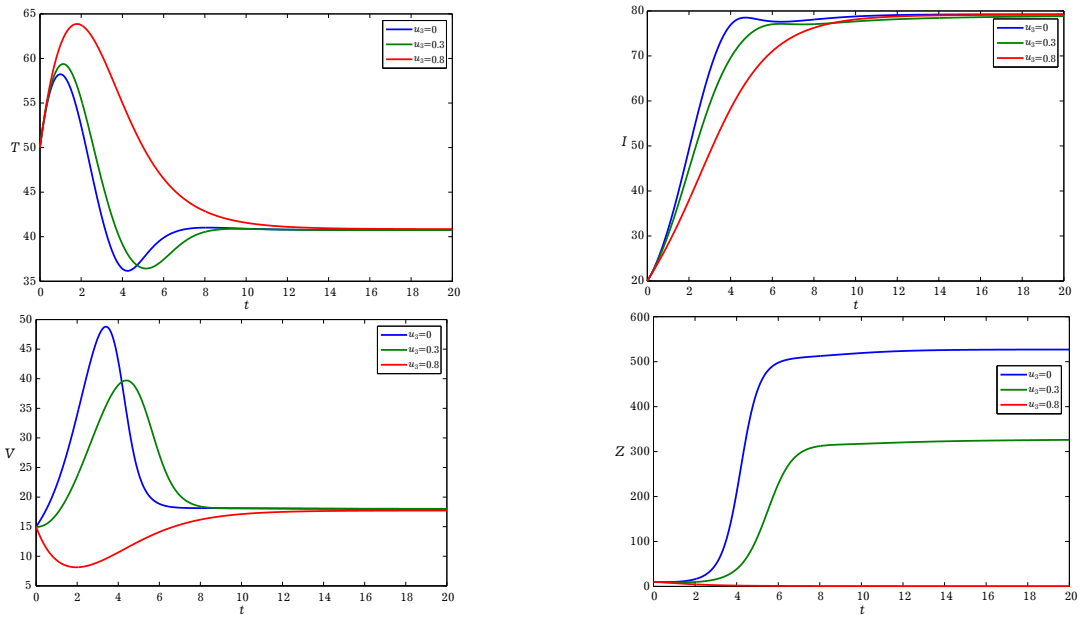

Fig. 13. Infection dynamics showing the stability of the E_2 for different values of u_3.

5.4. Effect of three therapies

In this subsection, we will study the effect of therapy parameters u_1, u_2 and u_3 used simultaneously, on the dynamics of the model system for each equilibrium.

Figures 14 and 15 show the behavior of the infection for the case of the free-equilibrium E_0 and endemic-equilibrium E_1 respectively, in the presence of therapy an increase of uninfected cells during is observed. However, a decrease of the infected cells and the virus load are observed.

Figures 16 confirm the result of the previous figure but also a significant decrease of the adaptive immune response is also observed. It is evident that higher doses of the medication lead to better results. It is worth noting that despite the theoretical effectiveness of these treatments, selecting the most suitable dosage for each patient is crucial to minimize potential adverse effects. For further insight, [26].

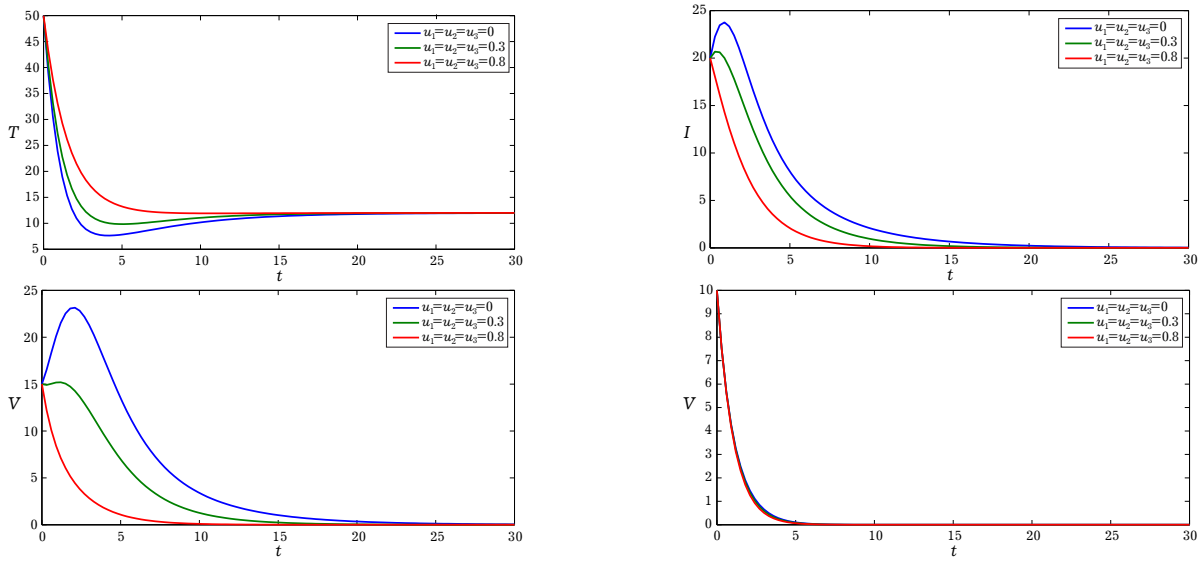

Fig. 14. Infection dynamics showing the stability of the equilibrium point E_0 for different values of u_1, u_2 and u_3 used simultaneously.

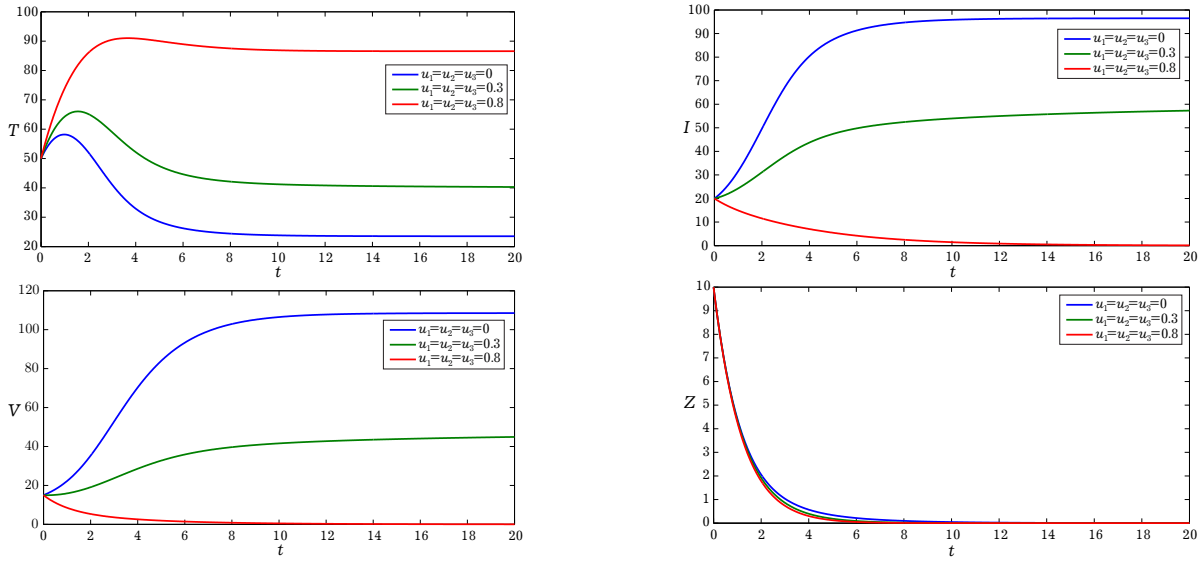

Fig. 15. Infection dynamics showing the stability of the equilibrium point E_1 for different values of u_1, u_2 and u_3 used simultaneously.

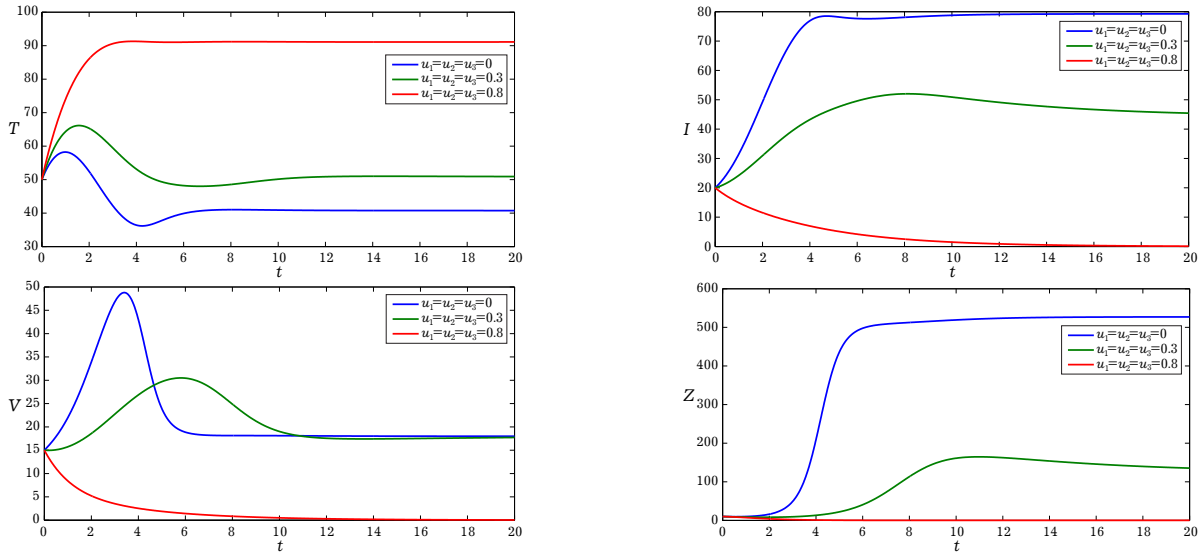

Fig. 16. Infection dynamics showing the stability of the equilibrium point E_2 for different values of u_1, u_2 and u_3 used simultaneously.

6. Conclusion

This paper is devoted to modeling the viral infection dynamics by the the ordinary differential equations describing the uninfected cells, infected cells, free virus and the humoral immune response, also the model under consideration includes the transmission between free virus to uninfected cells and other form of the transmission is by infected cells to uninfected cells namely cell-to-cell which incorporates both the cell-free and cell-to-cell transmission. Firstly, we have proven the Well-posedness of our mathematical model in terms of showing the existence, positivity and boundedness of solutions. Moreover, we determine the different equilibrium of the problem. Also, we studied the global stability of each equilibrium. Finally, we presented some numerical simulation in order to validate our theoretical findings, in the last part of our paper we gave some numerical recommendation of three therapies introduced to model, and we show that if the efficiency of the treatment reaches a 80%, we will maximize the number of the uninfected cells and minimize the number of the infected cells, the free virus

and the humoral immunity, that proves the crucial role of the treatment of the various viral infection and this can help a patient to increase the chance of the surviving. In the future work, we will study the effect of the memory infection on the treatment strategy, generated by the fractional derivative model [27–30]. Moreover, we will introduce on the studied model the stochastic perturbations in order to try the cases of the extinction and the persistence of the infection [31, 32].

[1] Burchell A. N., Winer R. L., de Sanjosé S., Franco E. L. Epidemiology and transmission dynamics of genital HPV infection. Vaccine. **24** (Suppl. 3), S52–S61 (2006).

[2] Elbasha E. H., Dasbach E. J., Insinga R. P. A multi-type HPV transmission model. Bulletin of Mathematical Biology. **70** (8), 2126–2176 (2008).

[3] Perelson A. S., Neumann A. U., Markowitz M., Leonard J. M., Ho D. D. HIV-1 dynamics in vivo: virion clearance rate, infected cell life-span, and viral generation time. Science. **271** (5255), 1582–1586 (1996).

[4] Adams B. M., Banks H. T., Davidian M., Kwon H.-D., Tran H. T., Wynne S. N., Rosenberg E. S. HIV dynamics: modeling, data analysis, and optimal treatment protocols. Journal of Computational and Applied Mathematics. **184** (1), 10–49 (2005).

[5] Wodarz D. Hepatitis C virus dynamics and pathology: the role of CTL and antibody responses. Journal of General Virology. **84** (7), 1743–1750 (2003).

[6] Sadki M., Danane J., Allali K. Hepatitis C virus fractional-order model: mathematical analysis. Modeling Earth Systems and Environment. **9**, 1695–1707 (2023).

[7] Danane J., Allali K., Hammouch Z. Mathematical analysis of a fractional differential model of HBV infection with antibody immune response. Chaos, Solitons & Fractals. **136**, 109787 (2020).

[8] Li M., Zu J. The review of differential equation models of HBV infection dynamics. Journal of Virological Methods. **266**, 103–113 (2019).

[9] Estrada E. COVID-19 and SARS-CoV-2. Modeling the present, looking at the future. Physics Reports. **869**, 1–51 (2020).

[10] Danane J., Hammouch Z., Allali K., Rashid S., Singh J. A fractional-order model of coronavirus disease 2019 (COVID-19) with governmental action and individual reaction. Mathematical Methods in the Applied Sciences. 46 (7), 8275–8288 (2023).

[11] Uçar E., Özdemir N., Altun E. Qualitative analysis and numerical simulations of new model describing cancer. Journal of Computational and Applied Mathematics. **422**, 114899 (2023).

[12] Nowak M. A., Bangham C. R. M. Population dynamics of immune responses to persistent viruses. Science. **272** (5258), 74–79 (1996).

[13] Dunia R., Bonnecaze R. Mathematical modeling of viral infection dynamics in spherical organs. Journal of Mathematical Biology. **67** (6), 1425–1455 (2013).

[14] Neumann A. U., Lam N. P., Dahari H., Gretch D. R., Wiley T. E., Layden T. J., Perelson A. S. Hepatitis C viral dynamics in vivo and the antiviral efficacy of interferon-α therapy. Science. **282** (5386), 103–107 (1998).

[15] Brimacombe C. L., Grove J., Meredith L. W., Hu K., Syder A. J., Flores M. V., Timpe J. M., Krieger S. E., Baumert T. F., Tellinghuisen T. L., Wong-Staal F., Balfe P., McKeating J. A. Neutralizing antibody-resistant hepatitis C virus cell-to-cell transmission. Journal of Virology. **85** (1), 596–605 (2011).

[16] Mojaver A., Kheiri H. Dynamical analysis of a class of hepatitis C virus infection models with application of optimal control. International Journal of Biomathematics. **9** (3), 1650038 (2016).

[17] Cao X., Roy A. K., Al Basir F., Roy P. K. Global dynamics of HIV infection with two disease transmission routes-a mathematical model. Communications in Mathematical Biology and Neuroscience. **2020**, 8 (2020).

[18] Sadki M., Harroudi S., Allali K. Dynamical analysis of an HCV model with cell-to-cell transmission and cure rate in the presence of adaptive immunity. Mathematical Modeling and Computing. **9** (3), 579–593 (2022).

[19] Reluga T. C., Dahari H., Perelson A. S. Analysis of hepatitis C virus infection models with hepatocyte homeostasis. SIAM Journal on Applied Mathematics. **69** (4), 999–1023 (2009).

[20] Alberts B., Johnson A., Lewis J., Raff M., Roberts K., Walter P. Molecular Biology of the Cell. Garland Science, New York (2002).

[21] Danane J., Allali K. Optimal control of an HIV model with CTL cells and latently infected cells. Numerical Algebra, Control and Optimization. **10** (2), 207–225 (2020).

[22] Hattaf K., Yousfi N. Two optimal treatments of HIV infection model. World Journal of Modelling and Simulation. **8** (1), 27–35 (2012).

[23] Van den Driessche P., Watmough J. Reproduction numbers and sub-threshold endemic equilibria for compartmental models of disease transmission. Mathematical Biosciences. **180** (1–2), 29-48 (2002).

[24] Chen S.-S., Cheng C.-Y., Takeuchi Y. Stability analysis in delayed within-host viral dynamics with both viral and cellular infections. Journal of Mathematical Analysis and Applications. **442** (2), 642–672 (2016).

[25] Hale J. K., Lunel S. M. V. Introduction to Functional Differential Equations. Applied Mathematical Sciences. Springer, New York (2013).

[26] Ait Ichou M., Bachraoui M., Hattaf K., Yousfi N. Dynamics of a fractional optimal control HBV infection model with capsids and CTL immune response. Mathematical Modeling and Computing. **10** (1), 239–244 (2023).

[27] Ghanbari B. A new model for investigating the transmission of infectious diseases in a prey-predator system using a non-singular fractional derivative. Mathematical Methods in the Applied Sciences. **44** (13), 9998–10013 (2021).

[28] Almeida R., Brito da Cruz A. M. C., Martins N., Monteiro M. T. T. An epidemiological MSEIR model described by the Caputo fractional derivative. International Journal of Dynamics and Control. **7**, 776–784 (2019).

[29] Bounkaicha C., Allali K., Tabit Y., Danane J. Global dynamic of spatio-temporal fractional order SEIR model. Mathematical Modeling and Computing. **10** (2), 299–310 (2023).

[30] Elkaf M., Allali K. Fractional derivative model for tumor cells and immune system competition. Mathematical Modeling and Computing. **10** (2), 288–298 (2023).

[31] Kiouach D., Sabbar Y. Dynamic characterization of a stochastic SIR infectious disease model with dual perturbation. International Journal of Biomathematics. **14** (04), 2150016 (2021).

[32] Rihan F. A., Alsakaji H. J. Analysis of a stochastic HBV infection model with delayed immune response. Mathematical Biosciences and Engineering. **18** (5), 5194–5220 (2021).

Модель вірусної інфекції з міжклітинною передачею та терапією за наявності гуморального імунітету: глобальний аналіз

Ель Акраа Н.[1], Лахбі М.[1], Данане Дж.[2]

[1] *Лабораторія математики та прикладних програм, Університет Хасана II, Вища педагогічна школа Касабланки, Касабланка, Марокко*

[2] *Лабораторія систем, моделювання та аналізу для підтримки прийняття рішень, Національна школа прикладних наук, Перший університет Хасана, Берречид, Марокко*

Ця стаття спрямована на моделювання математичної моделі вірусної інфекції, яка включає як безклітинну передачу, так і міжклітинну передачу. Модель включає чотири відділи, а саме: чутливі, інфіковані, вірусне навантаження та гуморальну імунну відповідь, яка активується в господаря для атаки на вірус. Спершу встановлено коректність запропонованої математичної моделі з точки зору доведення існування, додатності та обмеженості розв'язків. Крім того, визначено різні рівноваги задачі. Також досліджено глобальну стійкість кожної рівноваги. Накінець, проведено чисельне моделювання, щоб підтвердити теоретичні висновки та дослідити ефект різних типів лікування, які пропонуються в моделі.

Ключові слова: *глобальна стійкість; від клітини до клітини; гуморальна імунна відповідь; терапія; базовий номер відтворення; чисельне моделювання.*